Ferroelectrics, 348:19–24, 2007

ISSN: 0015-0193 print / 1563-5112 online
DOI: 10.1080/00150190701196013

Taylor & Francis
Taylor & Francis Group

Optical Multivibrator with Ferroelectric $Sn_2P_2S_6$

ALEXANDR SHUMELYUK,* ANDRIJ HRYHORASHCHUK, AND SERGUEY ODOULOV

Institute of Physics, National Academy of Sciences, 03 650 Kiev, Ukraine

*Periodic anharmonic modulation of output intensity is studied for semilinear coherent oscillator with photorefractive crystal that possesses two types of movable charge carriers. The pulse amplitude and modulation frequency are shown to depend considerably on grating spacing of photorefractive grating. We calculate these dependences within the model proposed earlier [*A. Shumelyuk, A. Hryhoraschuk, S. Odoulov, Phys Rev. A*, 72,* 023819 (2005)*] and show satisfactory agreement with the experimental data.*

Introduction

High refractive index changes at low intensities and intensity gain which is due to beam coupling effect are inherent features of photorefractive nonlinearity, typical for crystals lacking a symmetry center (see, e.g., [1]). For years after the discovery of photorefraction the main applications of this nonlinearity were considered in the fields of holographic optical memory and optical processing of information (including amplification of image bearing coherent light beams, real time interferometry, and phase conjugation). These applications profit from known advantage of photorefractive crystals that consists in intensity coupling of two beams that record an index grating what leads to the light amplification. At the same time, the photorefractive crystals themselves and, especially, photorefractive coherent oscillators [2] can be used for generating rather unusual temporal envelopes of the light field. Apart from cw oscillation with the frequency which is identical or slightly shifted with respect to that of the pump wave [3] these oscillators may show irregular pulsations that reveal deterministic chaos [4] or cosine modulation of the output intensity that points to multimode oscillation with two distinct temporal frequencies [5].

Recently we discovered a new, rather unusual mode of oscillation in ferroelectric $Sn_2P_2S_6$, with nearly saw-tooth modulation of output beam intensity and regular variation of the output beam phase between two discrete states separated to π from each other [6]. The origin of this operation mode which we call "optical multivibrator" is related to competition of two complimentary index gratings (shifted in space exactly to half grating spacing) that occurs in presence of two types of movable charge carriers, electrons and holes [7]. In this paper, after short description of the optical multivibrator we present the results of new measurements. It is shown that multivibrator mode of operation dominates in a wide

Received May 15, 2006.
*Corresponding author. E-mail: shumelyuk@iop.kiev.ua

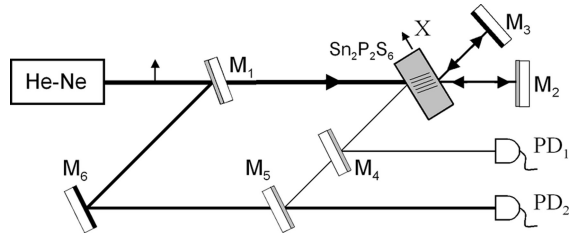

Figure 1. Schematic of the experimental set-up. The light beam from He-Ne laser is splitted into two beams by a semitransparent mirror M_1. A transmitted part serves as one of two counterpropagating pump beams; the other pump beam is formed by retroreflecting mirror M_2. The oscillation occurs in a cavity formed by photorefractive sample ($Sn_2P_2S_6$) and conventional highly reflecting mirror M_3. A semitransparent mirror M_4 directs a part of output oscillation wave to photodetector PD_1; the other part of oscillation wave, mixed with the reference wave from He-Ne laser by the mirror M_5 is sent to photodetector PD_2. Arrow shows the polarization of the pump beam.

spatial frequency range of the arising index gratings and the measured spatial frequency dependence of pulse duration can be reasonably explained within the proposed model.

Distinctive Features and Model of Optical Multivibrator

The semilinear coherent oscillator with two counterpropagating pump waves is studied. Figure 1 depicts schematically the experimental set-up. The output beam of TEM_{oo} He-Ne laser (633 nm, 40 mW) is sent to the $Sn_2P_2S_6$ sample and the transmitted beam is reflected back by a mirror M_2. With two counterpropagating pump waves the sample itself serves as phase conjugate mirror, it forms, with highly reflecting conventional mirror M_3, a semilinear coherent oscillator. The rectangular sample is cut along the crystastallographic axes and it measures $9 \times 4.5 \times 9$ mm^3. The sample is tilted in a way that the incidence angle of the pump beam is equal to 30°. This angle is kept the same in all experiments; the change of grating spacing Λ is achieved by variation of the oscillation wave incidence angle. The grating vector of the arising photorefractive grating is aligned roughly along the polar OX directions of $Sn_2P_2S_6$ sample. The pump waves are polarized in XOZ plane, light enters the sample through [001] faces.

The output intensity of the coherent oscillator is measured with the detector PD_1 while the detector PD_2 continuously monitors the temporal variations of interference signal of the oscillation wave with the coherent reference wave coming directly from He-Ne laser (see Fig. 1). The processing of these two signals (from PD_1 and PD_2) allows extracting the temporal variations of the oscillation wave intensity, amplitude and phase. A representative examples are shown in Fig. 2a, b, c, respectively. It is quite evident that the appearance of any new spike in oscillation wave is accompanied by a sudden change to π of the oscillation wave phase. These changes of phase are plotted directly in Fig. 2c, the change of the sign of the oscillation amplitude in every new spike (Fig. 2b) is also significant.

The described behavior of the oscillation output indicates that the photorefractive grating which is responsible for the oscillation wave changes its spatial position exactly to half of its spacing every time when oscillation intensity drops to zero. Treated in different terms the same effect consists in the contrast reversal of the photorefractive grating that occurs every time when new oscillation pulse develops. A detailed qualitative explanation of this type of oscillation is given in our publication [6]. We believe that only the fast grating (formed by photoexcited holes in $Sn_2P_2S_6$) is responsible for development of the first

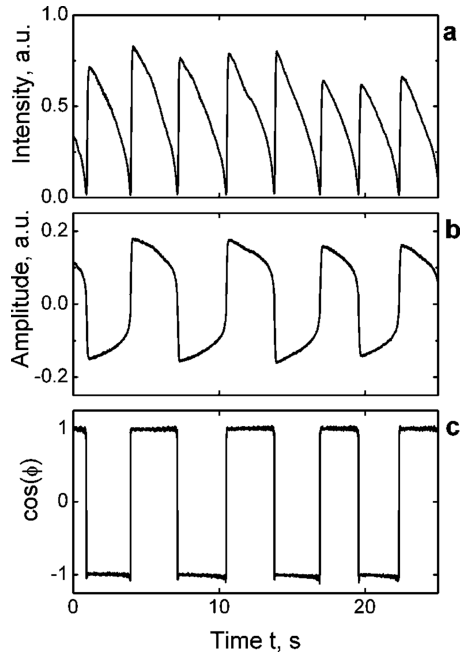

Figure 2. Fragment of already established temporal variations of the measured oscillation intensity (a) and reconstructed oscillation amplitude (b) and phase (c).

pulse of oscillation. Whenever this grating reaches its steady state value (coupling strength becomes $\Gamma\ell_{\mathrm{f}}$) the slow grating starts to develop, formed by thermally excited electrons in $Sn_2P_2S_6$. This grating is π-shifted with respect to the initial fast grating and therefore it decreases overall gain until it drops down to its threshold value (threshold coupling strength $\Gamma\ell_{\mathrm{th}}$). The oscillation disappears; the coupling strength associated with slow grating is at this moment $\Delta\Gamma\ell_{\mathrm{s}}$. Note that this value is smaller than ultimate saturated value for slow grating $\Gamma\ell_{\mathrm{s}}$ which is equal, in zeroth approximation, to that of the fast grating, $\Gamma\ell_{\mathrm{s}} = \Gamma\ell_{\mathrm{f}}$.

When the oscillation disappears the fast grating decays very quickly, within several milliseconds, while the slow grating remains practically unaffected, keeping the same amplitude $\Delta\Gamma\ell_{\mathrm{s}}$, because of its very long lifetime (on the order of one minute). This grating serves now as a very strong seed that initiates the development of a new fast grating which is exactly in phase with the seeding grating. New pulse of the oscillation intensity develops, π-shifted in phase with respect to the previous one. The maximum amplitude of the grating corresponds to the sum of two particular contributions (coupling strength $\Gamma\ell_{\mathrm{f}} + \Delta\Gamma\ell_{\mathrm{s}}$) [8]. After the maximum of this new grating is achieved the thermally excited electrons start to form an out-of-phase grating, its amplitude is growing until the overall gain reduces to the threshold value, the oscillation disappears and all further events repeat those already described.

Neglecting strong coupling effects (the influence of oscillation wave on space-charge field) and taking into account huge difference of the decay times $\tau_{\mathrm{s}} \gg \tau_{\mathrm{f}}$ (more than three orders of magnitude) we can expect that the duration of the oscillation pulse depends first of all on the rate with which the slow grating develops and on overthreshold coupling strength. If the slow grating grows exponentially the following relationship for pulse duration Δt holds:

$$(\Gamma\ell_{\mathrm{f}} + \Delta\Gamma\ell_{\mathrm{s}}) \exp(-\Delta t/\tau_{\mathrm{s}}) = \Gamma\ell_{\mathrm{th}}, \tag{1}$$

that leads to approximate expression for pulse duration

$$\Delta t \;=\; \tau_{\rm s} \ln\left[\frac{2\Gamma\ell_{\rm f} \;-\; \Gamma\ell_{\rm th}}{\Gamma\ell_{\rm th}}\right]. \tag{2}$$

It should be noted that the pulse period T consists of two consecutive spikes that differ in phase, i.e., $T = 2\Delta t$. In what follows we check to what extent Eq. 2 describes the experimentally measured dependence of T on the grating spacing Λ.

Experiment and Discussion

In this paper we study the oscillation behavior as a function of the grating spacing of the developing photorefractive grating. To characterize the used $Sn_2P_2S_6$ sample the saturation values of $\Gamma\ell_{\rm f}$ and $\Gamma\ell_{\rm s}$ were extracted from the dynamics of two-beam coupling, measured for different angles between the pump wave and oscillation wave, as also the decay times $\tau_{\rm f}$ and $\tau_{\rm s}$ were evaluated.

The coherent oscillation has been observed in a wide range of angles between the pump and oscillation waves from $\approx 11^\circ$ to $\approx 41^\circ$, i.e., in a range of grating spacing from 1.0 to 3.7 μm. Everywhere within this range the dynamics of oscillation is the optical-multivibrator type. The measured dependence of the modulation period versus grating spacing is shown in Fig. 3 (filled squares). The solid line represents the result of calculation as it will be explained in what follows.

Qualitatively the measured dependence agrees well with the prediction of Eq. 2: The closer we come to the oscillation threshold the shorter become oscillation pulses, with tendency to reach $T \to 0$ exactly at the threshold. To plot a dependence $T = T(\Lambda)$ one need to find first the grating spacing dependences of the decay time $\tau_{\rm f}$, $\tau_{\rm s}$ and coupling strengths $\Gamma\ell_{\rm f}$, $\Gamma\ell_{\rm s}$. It is necessary to estimate also how the threshold of oscillation varies when the direction of propagation of the pump wave is changing.

From the standard two-beam coupling experiments we measured first of all the grating spacing dependences of the coupling strengths $\Gamma\ell_{\rm f}$, $\Gamma\ell_{\rm s}$ shown in Fig. 4 by filled squares and empty dots, respectively. The data for fast grating were fitted by a well known dependence

$$\Gamma = -\frac{4\pi^2 n^3 \xi r_{\rm eff}}{\lambda\cos\psi}\frac{k_{\rm B}T}{e}\frac{\Lambda}{\Lambda^2+\ell_{\rm s}^2}, \tag{3}$$

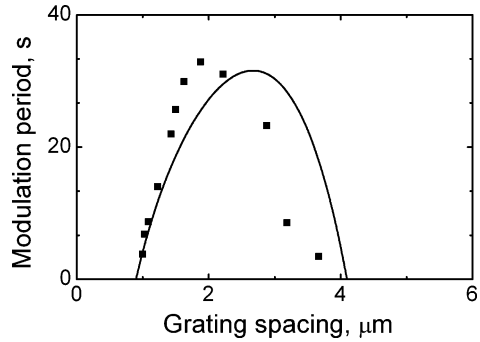

Figure 3. Grating spacing dependence of the modulation period T.

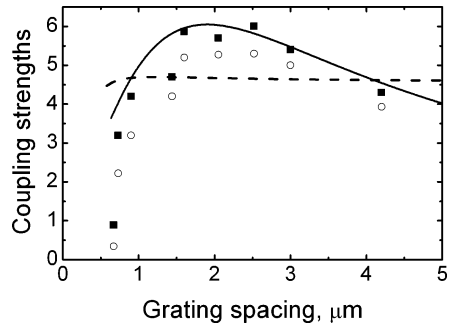

Figure 4. Grating spacing dependence of coupling strengths for fast and slow gratings (solid squares for $\Gamma\ell_f$ and empty dots for $\Gamma\ell_s$, respectively). Solid line represents best fit of theoretical dependence given by Eq. 3. Dashed line shows estimated changes of the threshold coupling strength (see text).

with n standing for the refractive index, the effective electrooptic constant ξr_{eff}, the Bolzmann constant k_B, the electron charge e, the light wavelength λ, the angle between pump and oscillation beams inside the sample ψ and the Debye screening length ℓ_s . From this fit we estimate the effective electrooptic coefficient of our sample $\xi r_{eff} = 53$ pm/V and Debye screening length $\ell_s = 1.9$ μm. The comparison of data for fast and slow gratings shows that $\Gamma\ell_s \approx 0.9\ \Gamma\ell_f$ what justifies the assumption taken when deriving Eq. 2.

By dotted line in Fig. 4 the calculated dependence of the threshold coupling strength is shown. It was obtained in a following way: For particular pump incidence angle that ensures grating spacing $\Lambda = 2$ μm the intensity of the transmitted through the sample light was measured and the pump ratio was calculated taking into account partial reflectivity of the mirror M_2 (R = 0.19). With the known pump ratio r and with the effective reflectivity of the cavity mirror M_3 (R = 0.98) the threshold coupling strength was found to be $\Gamma\ell_{th} \approx 4.7$. For all other values of grating spacing $\Gamma\ell_{th}$ was calculated taking into account changes caused by variation of Fresnel losses for transmitted pump wave. Maximum variation of $\Gamma\ell_{th}$ within the studied range of Λ was within 0.03 of the mean value.

From the data of Fig. 4 one can find the limit values of the grating spacing Λ where $\Gamma\ell_f = \Gamma\ell_{th}$ and beyond which the oscillation does not occur, 0.9 μm and 4 μm. The comparison with the data of Fig. 3 shows a satisfactory agreement of the estimates and experimental data.

Other dependence that is important for calculation of modulation period is the grating spacing dependence of slow grating decay time. This dependence was extracted from the same set of measurements of the oscillation dynamics, that was used for evaluation of $\Gamma\ell_f$ and $\Gamma\ell_s$. Figure 5 shows the results of measurements. The slow decay time increases with grating spacing roughly as Λ^2 while fast decay time becomes smaller with the increasing Λ.

With the data of Figs. 4 and 5 we have now all necessary information to plot the grating spacing dependence of the modulation period by using Eq. 2. The result is presented in Fig. 3 by the solid line. For the dependence calculated with no free parameter the agreement with the measured data is quite satisfactory. It might be improved further if slight difference in $\Gamma\ell_f$ and $\Gamma\ell_s$ will be taken into account in the model.

It is necessary to emphasize that the described temporal variation of the output oscillation intensity is drastically different both quantitatively and qualitatively from those related to Feinberg's frequency split at high values of coupling strength [9]. The modulation

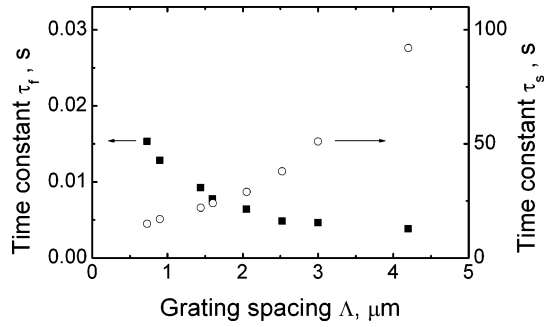

Figure 5. Grating spacing dependence of the decay times of the fast and slow gratings (τ_f and τ_s, respectively).

period, for example, decreases closer to the threshold for optical multivibrator while it goes to infinity exactly at bifurcation point in [9].

Acknowledgments

The authors are grateful to Dr. A. Grabar and Dr. I. Stoyka for $Sn_2P_2S_6$ sample used in this study. This work was supported in part within the Belarus-Ukraine Research Project # 10.01/022.

References

1. Photorefractive Materials and Their Applications. In: Gunter P., and Huignard J.-P., eds. Springer Series. New York: Springer Science+Business Media, Inc; 2005.
2. S. Odoulov, M. Soskin, and A. Khyzhnjak, Coherent Oscillators with Four Wave Mixing (Dynamic Grating Lasers) London, Chur: Harwood Academic Publishers; 1989.
3. B. Fischer, S. Sternklar, and S. Weiss, Photorefractive oscillators. *IEEE J. Quantum Electron*. **25**, 550–569 (1989).
4. R. L. Siuying, and G. J. Indebetouw, Periodic and chaotic spatiotemporal states in a phase-conjugate resonator using a photorefractive $BaTiO_3$phase-conjugate mirror. *Opt. Soc. Am. B*. **9**, 1507–1520 (1992).
5. A. Shumelyuk, S. Odoulov, and G. Brost, Multiline coherent oscillation in photorefractive crystals with two species of movable carriers. *Appl. Phys. B: Lasers Opt*. **68**, 959–966 (1999).
6. A. Shumelyuk, A. Hrygorashchuk, and Odoulov S: Coherent optical oscillator with periodic zero-π phase modulation. *Phys. Rev. A*. **72**, 023819 (2005).
7. S. Odoulov, A. Shumelyuk, U. Hellwig, R. Rupp, A. Grabar, and I. Stoika, Photorefraction in tin hypothiodiphosphate in the near infrared. *J. Opt. Soc. Am. B*. **13**, 2352–2360 (1996).
8. It should be emphasized that such a summation is possible only in case of limited trap density of the sample that imposes a restriction for space charge fields: $E_f + \Delta E_s \leq E_D$, E_D being the diffusion field.
9. P. Mathey, S. Odoulov, and D Rytz D, Instability of single-frequency operation in semilinear photorefractive coherent oscillatotr. *Phys. Rev. Lett*. **89**, 053901 (2002).